Deriving Predictive Relationships of Carotenoid Content at the Canopy Level in a Conifer Forest Using Hyperspectral Imagery and Model Simulation

Rocío Hernández-Clemente, Rafael Maria Navarro-Cerrillo, and Pablo J. Zarco-Tejada

***Abstract*—Recent studies have demonstrated that the R_{570}/R_{515} index is highly sensitive to carotenoid ($Cx+c$) content in conifer forest canopies and is scarcely influenced by structural effects. However, validated methods for the prediction of leaf carotenoid content relationships in forest canopies are still needed to date. This paper focuses on the simultaneous retrieval of chlorophyll ($Ca+b$) and ($Cx+c$) pigments, which are critical bioindicators of plant physiological status. Radiative transfer theory and modeling assumptions were applied at both laboratory and field scales to develop methods for their concurrent estimation using high-resolution hyperspectral imagery. The proposed methodology was validated based on the biochemical pigment quantification. Canopy modeling methods based on infinite reflectance formulations and the discrete anisotropic radiative transfer (DART) model were evaluated in relation to the PROSPECT-5 leaf model for the scaling-up procedure. Simpler modeling methods yielded comparable results to more complex 3-D approximations due to the high spatial resolution images acquired, which enabled targeting pure crowns and reducing the effects of canopy architecture. The scaling-up methods based on the PROSPECT-5+DART model yielded a root-mean-square error (RMSE) and a relative RMSE of 1.48 μg/cm^2 (17.45%) and 5.03 μg/cm^2 (13.25%) for $Cx+c$ and $Ca+b$, respectively, while the simpler approach based on the PROSPECT-5+Hapke infinite reflectance model yielded 1.37 μg/cm^2 (17.46%) and 4.71 μg/cm^2 (14.07%) for $Cx+c$ and $Ca+b$, respectively. These predictive algorithms proved to be useful to estimate $Ca+b$ and $Cx+c$ from high-resolution hyperspectral imagery, providing a methodology for the monitoring of these photosynthetic pigments in conifer forest canopies.**

***Index Terms*—Airborne, carotenoids, chlorophyll, conifers, forest, hyperspectral, R_{515}/R_{570}, R_{750}/R_{710}, scaling up, transformed chlorophyll absorption in reflectance index (TCARI)/optimized soil-adjusted vegetation index (OSAVI).**

Manuscript received June 5, 2013; revised September 30, 2013; accepted October 18, 2013. This work was supported in part by DIVERBOS under Grant CGL2011-30285-C02-02, by the University of Córdoba-Campus de Excelencia (Campus de Excelencia Internacional Agroalimentario–CEIA3), and by the Spanish Ministry of Science and Education (MEC) through the AGL2009-13105 project.

R. Hernández-Clemente and R. M. Navarro-Cerrillo are with the Escuela Técnica Superior de Ingeniería Agronómica y de Montes, Departamento de Ingeniería Forestal, Universidad de Córdoba, 14071 Córdoba, Spain (e-mail: rociohc@uco.es).

P. J. Zarco-Tejada is with the Instituto de Agricultura Sostenible, Consejo Superior de Investigaciones Científicas, 14004 Córdoba, Spain.

Color versions of one or more of the figures in this paper are available online at http://ieeexplore.ieee.org.

Digital Object Identifier 10.1109/TGRS.2013.2287304

I. Introduction

PHOTOSYNTHETIC pigments have been identified as important bioindicators of plant physiological state, mainly due to their roles in photosynthesis [1], [2]. Early diagnosis of forest decline processes has previously been made using photosynthetic pigment content as a stress indicator [3], [4]. The main short-term physiological response of trees undergoing decline is a general reduction in photosynthesis due to a large decrease in the levels of chlorophylls and carotenoids [5]. Several authors, e.g., Hoshizaki *et al.* [6] and Matyssek *et al.* [7], have demonstrated that the decline in chlorophyll content is associated with an increase in the values of the Ca/Cb ratio. By contrast, the $Ca+b/Cx+c$ ratio shows a decreasing trend under these conditions. Several authors [8], [9] have demonstrated that the increase of needle chlorosis and the decrease rate of carotenoid concentration are associated with the decline processes of conifer forest.

The aforementioned decrease in chlorophyll and carotenoid content in leaves leads to a lower overall absorption in the 430–700 nm region due to a reduction in the proportion of light-absorbing pigments. For this reason, several narrow-band optical indices have been reported to be sensitive to chlorophyll content at the leaf level (see [10] for a review of vegetation indices) and the canopy level [11]. Carotenoid-sensitive indices have been also analyzed, but they have received less attention. Although some authors have proposed indices sensitive to carotenoid pigment at the leaf level [12], [13], a recent study has explored their sensitivity when applied at the crown and canopy levels [14]. Despite the extensive work conducted on broadleaf species, strategies to link biochemical and optical properties in coniferous species have been limited by difficulties in measuring coniferous species. The main spectral region proposed for the retrieval of chlorophyll content is located in the red edge, where band ratios are highly sensitive to pigment content [15]. The red edge region shows the maximum slope in vegetation reflectance spectra, between 680 and 750 nm. This is because chlorophyll absorption is dramatically reduced from the red to the near-infrared region. In forest canopies, one of the most sensitive red edge formulations was found by Zarco-Tejada *et al.* [11], who demonstrated that the R_{750}/R_{710} red edge index was less sensitive than other chlorophyll indices to forest shadows, minimizing their disturbing effects on the retrieval of chlorophyll content. Later, the same red edge index formulation was also validated by other authors (e.g., Moorthy *et al.* [16] and

Zhang *et al.* [17]). Furthermore, combined indices sensitive to $Ca + b$ content have been developed. An example is the transformed chlorophyll absorption in reflectance index (TCARI) [18] combined with the optimized soil-adjusted vegetation index (OSAVI) [19], which minimizes soil effects and is robust for low leaf area index (LAI) levels in crops [18], [20]–[22]. Nevertheless, these potentially valuable indices that are suitable for field crops [18], olive orchards [21], and vineyards [20], [22] have not been validated for forest canopies, whose architecture varies substantially from that of agricultural areas.

Several methods have been proposed to retrieve biophysical parameters from hyperspectral reflectance in forest canopies, including scaling-up and model inversion methods that couple leaf and canopy transfer models [11], [16], [23]. Radiative transfer models have been widely used to simulate the bidirectional reflectance distribution of vegetation canopies considering different canopy complexities [24]. There are also simpler simulation approximations of the canopy such as infinite reflectance models [2], [25], [26]. Such models express an optically thick medium in terms of single reflectance and transmittance and consider different assumptions related to the scattering between layered leaves. A previous study reported by Zarco-Tejada *et al.* [11] suggested that these models are able to estimate the pigment content of broadleaf species in closed forests when pure crowns can be targeted using very high resolution imagery. Even under these conditions, the applicability of these simpler methods to the retrieval of pigment content in heterogeneous conifer forest canopies requires further research.

In an effort to model complex forest structures, 3-D models such as SPRINT [27], [28], FLIGHT [27], or discrete anisotropic radiative transfer (DART) [29] have been developed and evaluated [24]. The application of such models to simulate forest scenes, particularly the assessment of canopy-level indices for chlorophyll content estimation in conifers using PROSPECT [29] +SPRINT [23], yielded a root square error of 8.1 μg/cm^2 when targeting sunlit crown pixels. A more complex approach such as the DART model [30] was developed to simulate heterogeneous coniferous forests. As an example, the coupled PROSPECT+DART model was used by Malenovsky *et al.* [31] to estimate chlorophyll content using an artificial neural network, yielding a root square error of 2.95 μg/cm^2 when using the Area under curve Normalized to maximal Chlorophyll absorption Band depth between 650 and 720 nm method $(\mathrm{ANCB}_{650-720})$.

Despite the efforts made to assess several $Ca + b$-related vegetation indices, further research is needed to study $Cx + c$-sensitive indices both at the leaf and canopy levels. Moreover, both pigments exhibit overlapping absorption wavebands, increasing the difficulty of devising a nondestructive method for independently estimating pigment content in plants. For this purpose, we focused on the assessment of different narrow-band vegetation indices sensitive to $Cx + c$ in previous research [14]. In that study, the $\mathrm{R}_{515}/\mathrm{R}_{570}$ index was proposed for forestry sites, as it proved to be significantly related to leaf $Cx + c$ concentration both at leaf level ($\mathrm{r2} > 0.72$; $\mathrm{P} < 0.001$) and canopy level ($\mathrm{r2} > 0.71$; $\mathrm{P} < 0.001$), yet it was not possible to estimate $Cx + c$ using predictions or scaling-up relationships that accounted for the structure of the canopy. In forest sites, it is essential to be able to quantify $Ca + b$ and $Cx + c$ independently with sensitive narrow-band indices both at the leaf and canopy levels and develop predictive relationships. Therefore, the main focus of this paper was to develop a methodology specifically validated for heterogeneous forest canopies to simultaneously quantify $Ca + b$ and $Cx + c$ using scaling-up approaches rather than just assess the relationship between indices and carotenoid concentration. The study involved comparing modeling methods using the leaf PROSPECT model coupled with three infinite reflectance models (the simple approach) and a complex 3-D DART model for the retrieval of chlorophyll and carotenoid content at the crown level.

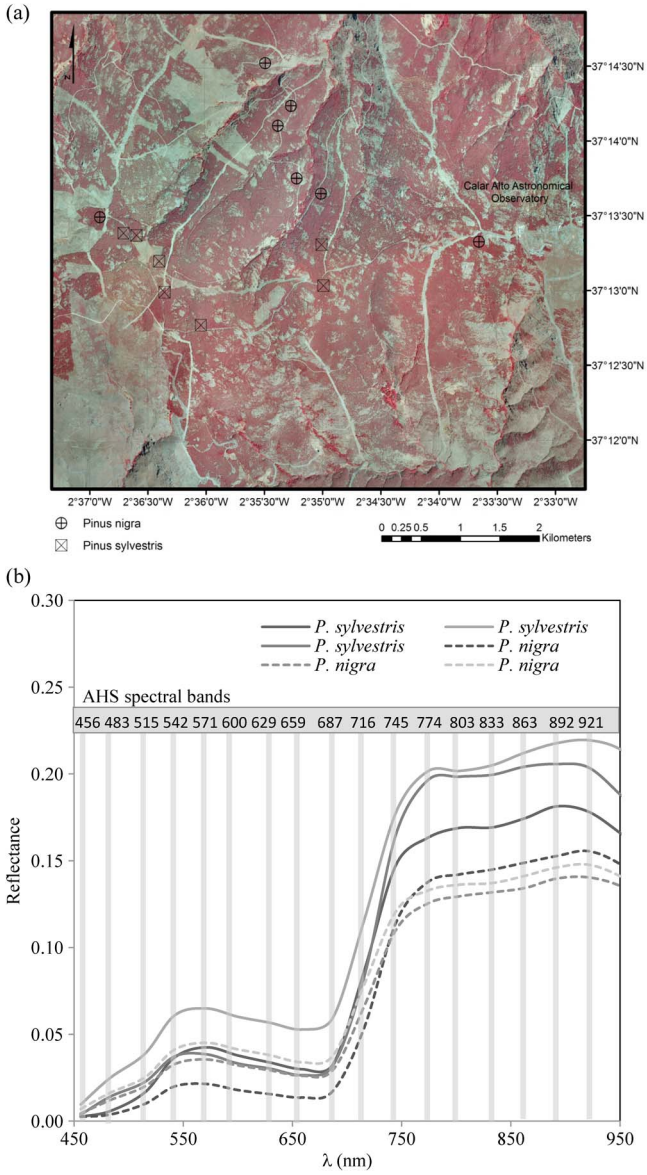

Fig. 1. (a) Overview of the area acquired with the AHS instrument and plot locations of the trees measured. (b) Single-pixel AHS spectra for pure-crown pixels of *P. sylvestris* and *P. nigra*.

II. Methods

A. Field Experiments and Data Collection

Field data collection was conducted in August 2008 in Sierra de Filabres (Almeria province, southeastern Spain) $(37°13'27''\mathrm{N}, 2°32'54''\mathrm{W})$ [see Fig. 1(a)], the driest region in

TABLE I
VARIABILITY RANGES OF MEASURED PARAMETERS FOR THE CONIFER FOREST SITES. MEAN. STANDARD DEVIATION (SD). MINIMUM AND MAXIMUM VALUES OF *P. sylvestris* (PS) AND *P. nigra* (PN)

		Mean		SD		Minimum		Maximum	
		Ps	Pn	Ps	Pn	Ps	Pn	Ps	Pn
Diameter at breast height	DBH (cm)	16.8	15.6	2.6	2.8	11.3	11.3	21	22
Tree height	H (m)	7.9	7.4	1.4	1.8	5.8	4.3	11.6	11.3
Crown diameter	Cd (m)	4.5	3.8	0.7	0.8	3.1	2.1	5.8	5.3
Crown height	Ch (m)	5.8	5.8	1.4	1.5	3.4	2.7	10.2	9.4
Basal area	BA ($m^2\,ha^{-1}$)	155.7	128.5	99.9	52	73.9	67.9	611	353
Stand density	SD (trees ha^{-1})	1050	925	418	353	100	100	1800	1600

Western Europe. The elevation of the study area ranged from 1540 to 2000 m.a.s.l., and the annual rainfall ranged between 300 and 400 mm. The annual average temperature was 11 °C, reaching a maximum of 32 °C in summer and a minimum of −8 °C in winter. The vegetation consisted of a 40-year-old pine afforestation of *Pinus nigra* Arnold (Black pine) and *Pinus sylvestris* L. (Scotch pine) (see Table I). Forest decline processes have been previously reported in Sierra de Filabres [32]. The field sampling campaigns were conducted concurrently with airborne overflights during the last week of July 2008. Needles were collected from the top of the crown by selecting branches of illuminated areas from a total of 21 trees. Needles were frozen in liquid nitrogen in the field and later stored at −80 °C prior to the determination of chlorophyll a and b and carotenoids. The mean crown pigment was calculated from a total of ten young needles (one-year-old needles) collected from the top of the crown.

Needle pigment concentration was determined as reported by Abadía and Abadía [33]. Pigment extracts were obtained from a mixed sample of 5 cm of needle material, using 1 linear cm per needle. The area was calculated by assuming that the needle was a half cylinder and the diameter was the measured width of each needle. The needle diameter was measured with a digital caliper precision instrument. Five additional needle samples were used to take structural measurements (thickness and width) to determine water content and dry mass. The needles were ground in a mortar on ice with liquid nitrogen and diluted in acetone up to 5 mL (in the presence of Na ascorbate). After that, the extracts were filtered through a 0.45-μm filter to separate the pigment extracts from the Na ascorbate. Spectrophotometric determinations were then conducted on the same extracts.

B. Airborne Campaigns

The airborne campaign was conducted by the Spanish National Institute of Aerospatial Technology (INTA) with an Airborne Hyperspectral Scanner (AHS) (Sensytech Inc., currently Argon St. Inc., Ann Arbor, MI, USA) in the last week of July 2008. Airborne data were obtained at 12:00 GMT, acquiring 2-m spatial resolution imagery in 38 bands in the 0.43–12.5-μm spectral range. The field of view (FOV) and instantaneous FOV of the AHS sensor were 90° and 2.5 mrad, respectively, and the study plots were imaged in the central region of the scene to avoid edge effects. At-sensor radiance processing and atmospheric correction were performed at the INTA facilities. Atmospheric correction was conducted with ATCOR4 based on the MODTRAN radiative transfer model, using aerosol optical depth measured at 550 nm with a Micro-Tops II sun photometer (Solar Light, Philadelphia, PA, USA) at the time of the flight.

The hyperspectral imagery acquired enabled the pure-crown identification of Scotch pine and Black pine [see Fig. 1(b)]. Single-crown reflectance spectra were extracted using a multiresolution segmentation strategy, which utilizes a region growing approach to spatially cluster pixels based on their similar NDVI values obtained from the hyperspectral imagery [see Fig. 2(a)–(c)]. This made it possible to extract the mean hyperspectral reflectance for sunlit and shaded crown components [see Fig. 2(d)]. Vegetation indices (see Table II) were calculated from the crown spectra for the retrieval of chlorophyll $Ca+b$ and carotenoid content $Cx+c$. The $Ca+b$-related vegetation indices were selected based on previous studies in forest canopies, using simple ratio indices located in the red edge region [11], [16] and including recent $Ca+b$-related indices validated for crop canopies such as the TCARI/OSAVI [18]. The $Cx+c$-sensitive vegetation index used was based on previous work where the R_{515}/R_{570} index was proposed by Hernández-Clemente *et al.* [14] and proved to be significantly related to the $Cx+c$ concentration both at the leaf ($r^2 > 0.72$, $p < 0.001$) and canopy ($r^2 > 0.71$, $p < 0.001$) levels.

C. Modeling the Retrieval of Chlorophyll and Carotenoid Content

The PROSPECT-5 model was used to simulate needle reflectance and transmittance for varying chlorophyll $Ca+b$ (10–60 μg/cm^2), carotenoid $Cx+c$ (2–16 μg/cm^2), and leaf water (0.01–0.03 cm) content and fixed values of dry matter content and leaf internal structure. Previous studies [16], [23] have demonstrated the feasibility of the PROSPECT model to simulate the reflectance and transmittance of needles compared to other specific conifer models such as LIBERTY [34]. Table III summarizes the nominal values used for leaf-level modeling. Fig. 3 shows the simulated spectral response obtained for $Cx+c$ variation, between 2 and 16 μg/cm^2, and $Ca+b$ values of 15 and 45 μg/cm^2 [see Fig. 3(a) and (b)]. Both figures show the specific absorption produced by the carotenoid in the spectral region from 500 to 550 nm. The effect of $Ca+b$ content variation on the R_{515}/R_{570} carotenoid index calculated at the leaf level is also shown in detail [see Fig. 3(c) and (d)]. These figures show that R_{515}/R_{570} is affected by chlorophyll concentration variation.

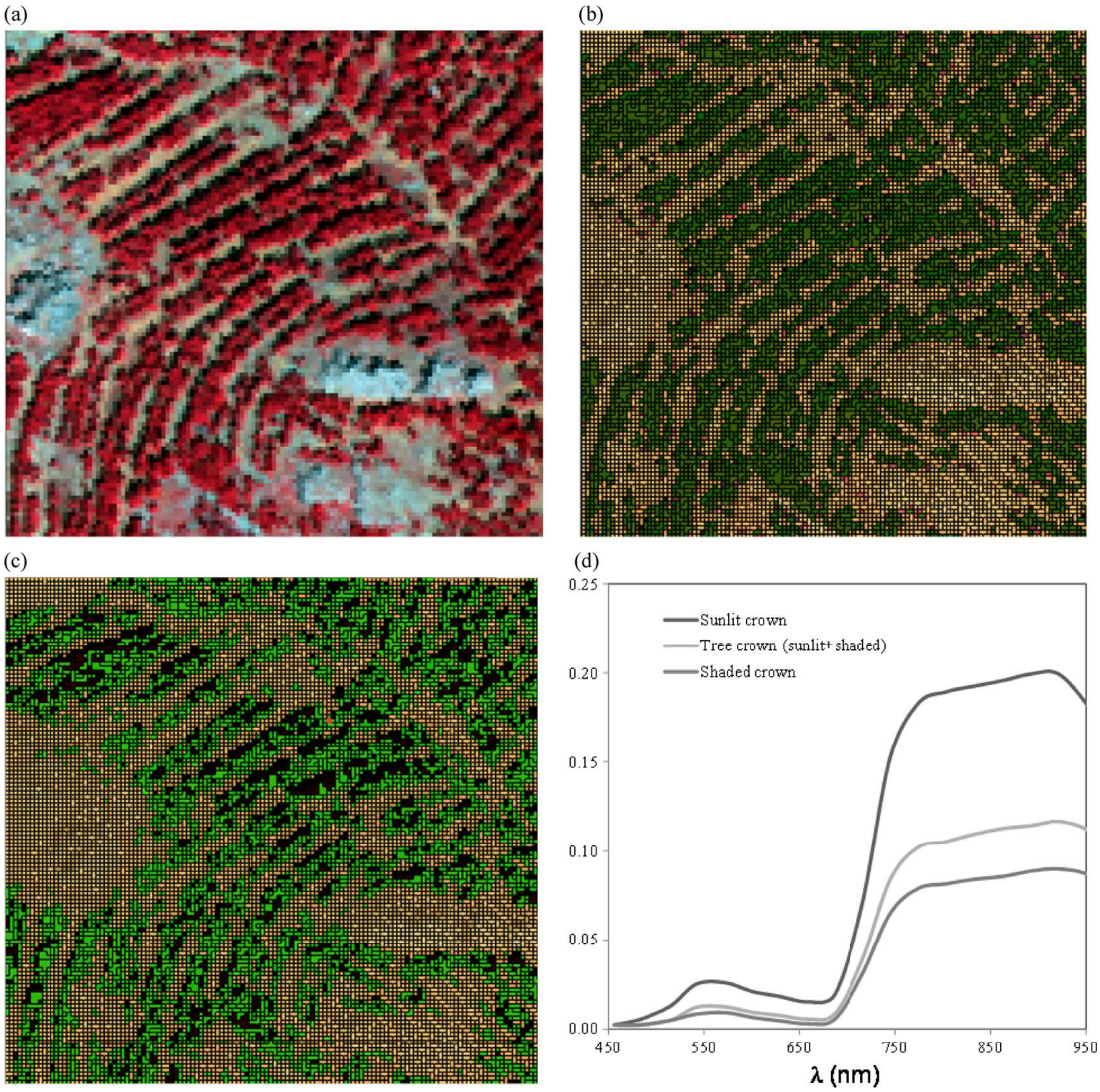

Fig. 2. (a) Overview of the area acquired with the AHS instrument. (b) Automatic object-based crown segmentation applied to the hyperspectral imagery. (c) Automatic object-based crown detection algorithm applied to the hyperspectral imagery to identify pure-crown extraction. Single-pixel AHS spectra for sunlit crown. (d) Tree crown (sunlit + shaded) and shaded crown.

TABLE II
NARROW-BAND OPTICAL VEGETATION INDICES APPLIED FOR CHLOROPHYLL AND CAROTENOID ESTIMATION AT LEAF LEVEL (L) AND CANOPY LEVEL (C)

Chlorophyll content			Reference	
Red Edge Chlorophyll Index	$CI_{red\ edge}$	R_{750}/R_{710}	[21]	L/C
Transformed Cab Absorption in Reflectance Index	TCARI	$3*[(R_{700}-R_{670})-0.2*(R_{700}-R_{550})*(R_{700}/R_{670})$	[18], [20]	L/C
Optimized Soil-Adjusted Vegetation Index	OSAVI	$(1+0.16)*(R_{800}-R_{670})/(R_{800}+R_{670}+0.16)$	[19], [20]	L/C
Carotenoid content			Reference	
Carotenoid simple ratio	CSR	R_{515}/R_{570}	[14]	L/C

The simulated leaf reflectance and transmittance spectra were used as input for the canopy radiative transfer simulations proposed in this paper. The scaling-up analysis was conducted by comparing the accuracy obtained with different canopy reflectance approximations to evaluate the suitability of each model for simultaneous chlorophyll and carotenoid pigment content retrieval. To achieve this purpose, scaling-up methods were first evaluated based on simpler formulas based on infinite reflectance R_{∞} simulations, which did not account for the canopy structure and the viewing geometry effects. The use of this type of models is justified in the high-resolution imagery chosen, which enabled the identification of pure-crown vegetation pixels.

After that, a more complex 3-D canopy reflectance radiative transfer model was analyzed and compared to the previous modeling results. This approach has successfully been tested in several studies [23], [31] and aims at estimating canopy biochemistry with simpler methods, minimizing structural effects through robust indices using models with a reduced number of inputs. The R_{∞} formulations used in this paper were based on the following: 1) $(R_{\infty 1})$ [2]; 2) $(R_{\infty 2})$ [26]; and 3) $(R_{\infty 3})$ [25]. Each formulation is based on different assumptions related to the scattering between layered leaves forming the optically thick canopy. $R_{\infty 1}$ and $R_{\infty 2}$ correspond to optically thick stacks of leaves in which multiple reflectance between leaves is

TABLE III
NOMINAL VALUES USED FOR LEAF AND CANOPY MODELING PARAMETRIZATION WITH PROSPECT-5 AND DART

PROSPECT-5	*Nominal values and ranges*
Chlorophyll a+b. C_{a+b} *(μg cm^{-2})*	10-60
Carotenoid content. C_{x+c} *(μg cm^{-2})*	2-16
Leaf water content. C_w *(cm)*	0.01-0.03
Leaf dry matter content. C_m *(g cm^{-2})*	0.03
Leaf internal structure parameter. *N*	2-3
DART	*Nominal values and ranges*
Central wavelength. *(nm)*	400-800
Spectral bandwidth. *(nm)*	10
Scene parameters	*Value*
Cell size. *(m)*	0.5
Scene dimensions. *(m)*	50 x 50
Spatial distribution	Random
Number of trees	1200 trees/ha
Soil reflectance	Image extracted
Probability of presence	0.8
Leaf area index (varied parameter)	1-7
Crown shape	Truncated cone
Crown height (mean). *(m)*	6
Crown height (SD.). *(m)*	0.9
Height below crown (mean). *(m)*	4
Height below crown (std. dev.). *(m)*	0.8
Diameter below crown (mean). *(m)*	0.4
Diameter below crown (std. dev.). *(m)*	0.1
Height within the tree crown. *(m)*	5
Diameter within the tree crown. *(m)*	0.35

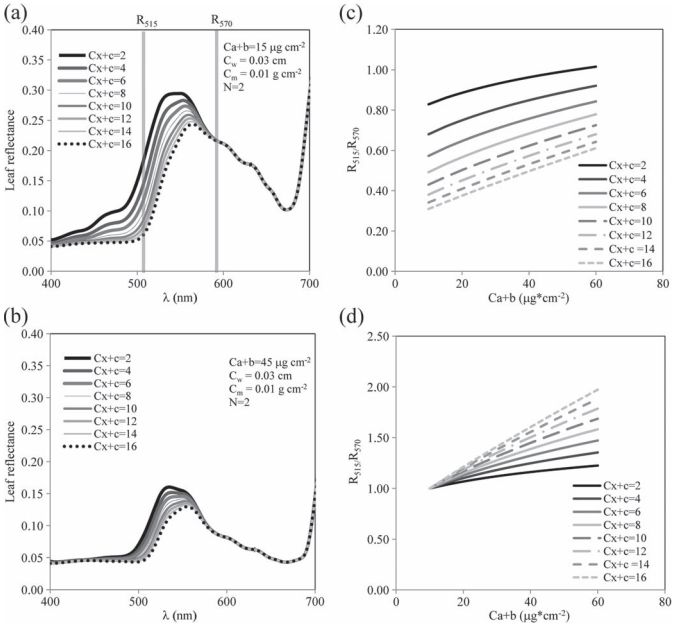

Fig. 3. Leaf-level modeling simulations conducted with the PROSPECT-5 model to assess the effects of $Cx + c$ and $Ca + b$ content on the spectral signature in the 400–700 nm spectral range. Simulations performed for $Cx + c$ variation between 2 and 16 μg/cm^2 and $Ca + b$ values of (a) 15 μg/cm^2 and (b) 45 μg/cm^2. (c) Simulated R_{515}/R_{570} spectral index obtained for $Cx + c$ variation between 2 and 16 μg/cm^2 and $Ca + b$ values from 10 to 60 μg/cm^2 and (d) the normalized variation of the simulated R_{515}/R_{570} spectral index.

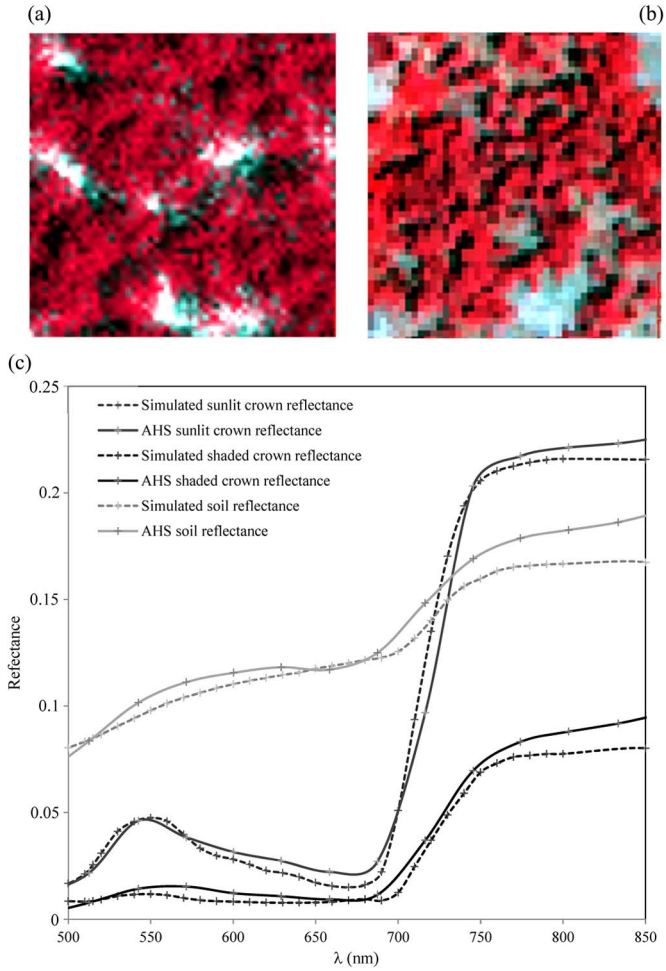

Fig. 4. PROSPECT-5+DART simulated image. (a) High-resolution multispectral image acquired with the AHS sensor. Tree crown and soil spectral reflectance obtained from (b) the multispectral image and (c) the simulated image.

ignored, whereas R∞3 characterizes the optically thick medium with single-leaf absorption and isotropic scattering properties. In addition, the 3-D DART model [30], [35] was used to simulate 3-D vegetation canopies. The DART model has been used to simulate forest canopy reflectance in Norway spruce (*Picea abies*), to retrieve chlorophyll content [31], and in Scotch pine canopies, to analyze $Cx + c$-related vegetation indices [14]. In this paper, the DART model was used to simulate canopy scenes modeling pure-crown reflectance in Scotch and Black pine canopies. These high-resolution 3-D simulations enabled the extraction of simulated sunlit crown reflectance from single trees. The 3-D forest scenes were built using various structural inputs within the range of variation (see Table III) observed from field measurements conducted at the study sites. Fig. 4 shows a sample area acquired with airborne hyperspectral imagery [see Fig. 4(a)] and the corresponding DART scene simulation [see Fig. 4(b)]. The airborne-AHS and DART-simulated spectra for sunlit and shaded crown reflectance are also shown [see Fig. 4(c)].

We used a data set of spectral canopy reflectance generated from the DART radiative transfer model and the three infinite reflectance models proposed to obtain predictive relationships between $Ca + b$ and $Cx + c$ and the TCARI/OSAVI,

TABLE IV
SIMULATION RESULTS OBTAINED FOR CROWN CAROTENOID CONTENT ($Cx+c$) RETRIEVAL WITH PROSPECT-5 AND DIFFERENT CANOPY APPROXIMATIONS THROUGH INFINITIVE REFLECTANCE R_∞ FORMULATIONS AND DART. RESULTS EXPRESSED AS [$R^2 \cdot$ RMSE(μg/cm^2)]

CANOPY APPROXIMATIONS		PROSPECT-5 +$R_{\infty 1}$		PROSPECT-5 +$R_{\infty 2}$		PROSPECT-5 +$R_{\infty 3}$		PROSPECT-5 +DART	
Regression models for the estimation of $Cx+c$ and $Ca+b$ content	Equation	R^2	RMSE (μg/cm^2)	R^2	RMSE (μg/cm^2)	R^2	RMSE (μg/cm^2)	R^2	RMSE (μg/cm^2)
$Cx+c=f(R_{515}/R_{570})$	1a	0.77	2.11	0.77	2.11	0.72	2.28	0.62	2.44
$Cx+c=f(R_{515}/R_{570}; (R_{750}/R_{710})^2)$	1b	0.91	1.35	0.91	1.36	0.79	1.86	0.81	1.7
$Cx+c=f(R_{515}/R_{570}; (R_{750}/R_{710})^2)$; TCARI/OSAVI)	1c	0.99	1.45	0.88	1.45	0.89	1.42	0.83	1.6

TABLE V
SIMULATION RESULTS OBTAINED FOR CROWN CHLOROPHYLL CONTENT ($Ca+b$) RETRIEVAL WITH PROSPECT-5 AND DIFFERENT CANOPY APPROXIMATIONS THROUGH INFINITIVE REFLECTANCE R_∞ FORMULATIONS AND DART. RESULTS EXPRESSED AS [$R^2 \cdot$ RMSE(μg/cm^2)]

CANOPY APPROXIMATIONS		PROSPECT-5 +$R_{\infty 1}$		PROSPECT-5 +$R_{\infty 2}$		PROSPECT-5 +$R_{\infty 3}$		PROSPECT-5 +DART	
Regression models for the estimation of $Cx+c$ and $Ca+b$ content	Equation	R^2	RMSE (μg/cm^2)	R^2	RMSE (μg/cm^2)	R^2	RMSE (μg/cm^2)	R^2	RMSE (μg/cm^2)
$Ca+b=f(R_{750}/R_{710})$	2a	0.92	4.55	0.92	5.26	0.95	8.21	0.82	6.08
$Ca+b=f(R_{750}/R_{710}; (R_{750}/R_{710})^2)$	2b	0.93	4.41	0.93	4.47	0.95	5.51	0.86	5.34
$Ca+b=f$(TCARI/OSAVI; TCARI/OSAVI)^2)	2c	0.8	6.97	0.88	6.97	0.84	6.04	0.8	6.97

R_{750}/R_{710}, and R_{515}/R_{570} indices. The database of synthetic spectra was generated using 250 simulations with random inputs for $Ca+b$, $Cx+c$, N, LAI, soil reflectance, and Cm (nominal values are shown in Table III). In total, 150 synthetic spectra were used for modeling, conducted with infinite reflectance formulas and through DART canopy simulations. We used 100 additional synthetic spectra to evaluate the root-mean-square error (RMSE) and the relative RMSE obtained for each scaling-up approach. The regression analyses between $Ca+b$, $Cx+c$, and the sensitive indices were based on quadratic models. The R_{515}/R_{570}, R_{750}/R_{710}, and TCARI/OSAVI indices were included as shown in

$$Cx+c = \mathrm{f}(R_{515}/R_{570}) \quad (1a)$$

$$Cx+c = \mathrm{f}\left(R_{515}/R_{570}, (R_{515}/R_{570})^2, R_{750}/R_{710}\right) \quad (1b)$$

$$Cx+c = \mathrm{f}\left(R_{515}/R_{570}, (R_{515}/R_{570})^2, \mathrm{TCARI/OSAVI}\right) \quad (1c)$$

$$Ca+b = \mathrm{f}(R_{750}/R_{710}) \quad (2a)$$

$$Ca+b = \mathrm{f}\left(R_{750}/R_{710}, (R_{750}/R_{710})^2\right) \quad (2b)$$

$$Ca+b = \mathrm{f}\left(\mathrm{TCARI/OSAVI}, (\mathrm{TCARI/OSAVI})^2\right). \quad (2c)$$

III. RESULTS

A. Modeling Results

The relationships obtained between the simulations conducted with the different approximations through infinite reflectance R_∞ models and the coupled PROSPECT-5+DART models yielded significant results ($p < 0.001$) for $Cx+c$ and $Ca+b$ estimation.

The predictive power of the different canopy approximations applied for the retrieval of pigment content ($Ca+b$ and $Cx+c$) yielded coefficients of determination ranging from $r^2 = 0.6$ to $r^2 = 0.9$ for both $Cx+c$ (see Table IV) and $Ca+b$ (see Table V). $R_{\infty 1}$ and $R_{\infty 2}$ showed slightly better performance than $R_{\infty 3}$ formulations for both $Cx+c$ (see Table IV) and $Ca+b$ (see Table V). As regards $Cx+c$ retrieval, the best RMSE values (RMSE $= 1.35$) were obtained by using scaling-up methods based on the model regression (1b) (see Table IV). We observed a consistent improvement in predictive power when using models (1b) and (1c) compared to model (1a). The differences between these results are explained because models (1b) and (1c) considered chlorophyll effects for carotenoid estimation by using both $Cx+c$- and $Ca+b$-sensitive vegetation indices in scaling-up relationships. As an example of the predictive power of the indices applied, the RMSE obtained with the $R_{\infty 1}$ scaling method was 2.11 μg/cm^2 (14.73%) using only the simple R_{515}/R_{570} ratio [model (1a)] and 1.35 μg/cm^2 (10.71%) using the R_{515}/R_{570} and R_{750}/R_{710} vegetation indices simultaneously [model (1b)] (see Table IV). For $Ca+b$ retrieval, the best coefficient of determination and RMSE values were also obtained by using the $R_{\infty 1}, R_{\infty 2}$ scaling methods and model (2b) (see Table V). The simulation demonstrated that the overall RMSE obtained using the R_{750}/R_{710} index was lower than that obtained using the TCARI/OSAVI. When the $R_{\infty 1}$ scaling-up method was used, the RMSE improved from 6.97 to 4.41 (μg/cm^2) (15.22 to 9.58%) (see Table V). Among the different canopy reflectance approximations, the use of quadratic equations based on the R_{750}/R_{710} index [model (2b)] successfully improved the RMSE values of the estimated $Ca+b$ content.

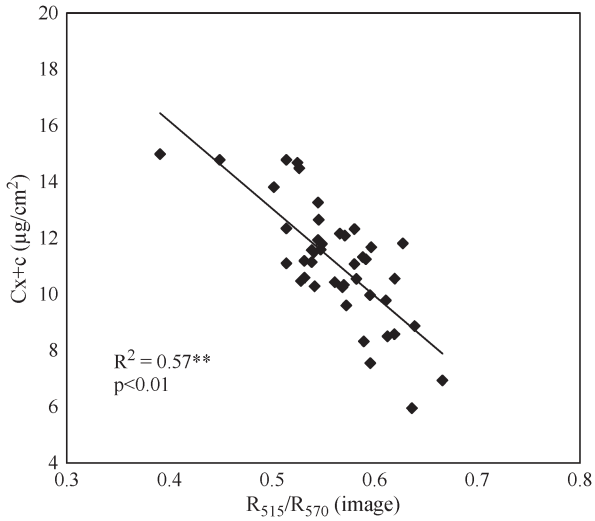

Fig. 5. Relationships obtained at the crown level between the R_{515}/R_{570} index obtained from the airborne hyperspectral imagery and field-measured $Cx + c$ for *P. sylvestris* and *P. nigra*.

Using 3-D model simulations, the best results for the estimation of $Cx + c$ were also obtained using the R_{515}/R_{570} and R_{750}/R_{710} vegetation indices simultaneously (1b); the best results for the estimation of $Ca + b$ were obtained using the R_{750}/R_{710} vegetation index (2b). A comparison of results obtained with the infinite reflectance models and 3-D model simulations showed similar values in both cases. For example, when a simpler approach such as the $R_{\infty 1}$ was used, results yielded an RMSE of 1.35 μg/cm^2 (10.71%) for $Cx + c$ and 4.41 μg/cm^2 (9.58%) for $Ca + b$; when the 3-D DART model was used, the RMSE was 1.7 μg/cm^2 for $Cx + c$ (11.31%) and 5.31 μg/cm^2 (11.50%) for $Ca + b$.

B. Experimental Results

The R_{515}/R_{570}, R_{750}/R_{710}, and TCARI/OSAVI indices were assessed as a first approach with the airborne imagery to study their sensitivity to $Ca + b$ and $Cx + c$ measured from the study sites. The relationship between $Cx + c$ content and R_{515}/R_{570} extracted from single crowns identified in the airborne imagery showed significant results ($p < 0.01$), yielding $r^2 = 0.57$ for the Scotch and Black pine aggregated samples (see Fig. 5). The relationships between $Ca + b$ content and the R_{750}/R_{710} [see Fig. 6(a)] and TCARI/OSAVI indices [see Fig. 6(b)] showed that the coefficient of determination was higher for the R_{750}/R_{710} index ($r^2 = 0.63$) than for the TCARI/OSAVI ($r^2 = 0.5$). In fact, the TCARI/OSAVI was more affected by the crown structure than the R_{750}/R_{710} index ($p < 0.01$ in both cases).

$Ca + b$ and $Cx + c$ content was then estimated by scaling up the optical indices using the prediction algorithms developed in the previous section. The models obtained from the simulation analysis (see Tables IV and V) were applied using the pure-crown reflectance extracted from the airborne imagery for each study site. Table VI shows the results obtained for the estimation of both $Ca + b$ and $Cx + c$ pigments at canopy level for Scotch pine stands using the four modeling approximations used and the different indices assessed.

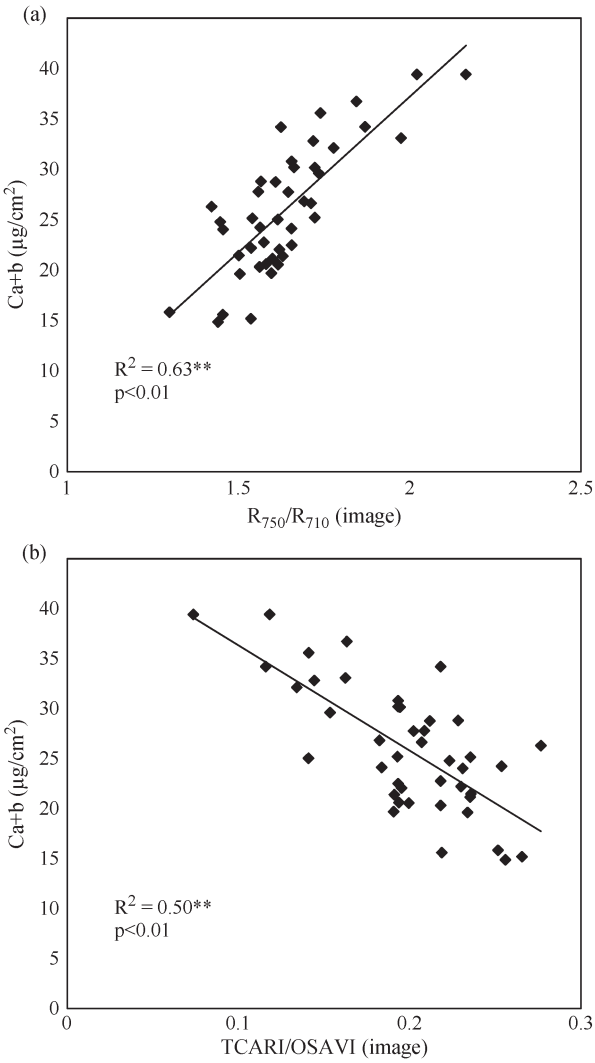

Fig. 6. Relationships obtained at the crown level between $Ca + b$ content and (a) the red edge index and (b) the TCARI/OSAVI index. Vegetation indices calculated from the airborne hyperspectral imagery and field-measured pigment content for *P. sylvestris* and *P. nigra*.

According to the results, among all the canopy approximations studied, the estimation of $Cx + c$ yielded an RMSE ranging from 1.35 to 2.12 μg/cm^2 (16.94%–21.028%) when using quadratic models based on the R_{515}/R_{570} and R_{750}/R_{710} indices (see Table VI). The model performance for $Ca + b$ using the R_{750}/R_{710} index yielded an accuracy ranging between 4.41 and 9.04 μg/cm^2 (13.67%–24.57%). Although the best results were obtained when PROSPECT-5 was coupled to DART (RMSE $= 4.41$ μg/cm^2 (13.67%) for $Ca + b$ and RMSE $= 1.35$ μg/cm^2 (12.52%) for $Cx + c$), results obtained using the simpler $R_{\infty 3}$ approach obtained comparable results [RMSE $= 5.5$ μg/cm^2 for $Ca + b$ (32.48%) and RMSE $= 1.45$ μg/cm^2 for $Cx + c$ (16.94%)]. The analysis carried out by introducing the TCARI/OSAVI into the model for both $Cx + c$ and $Ca + b$ pigment retrieval showed significantly worse results, yielding poorer RMSE values for all models. Using the TCARI/OSAVI index, the best results obtained for Scotch pine stands through the $R_{\infty 3}$ infinite reflectance simulation yielded values of RMSE $= 22.76$ and 4.78 μg/cm^2 for $Ca + b$ and $Cx + c$ estimations, respectively.

TABLE VI
COEFFICIENTS OF DETERMINATION AND RMSE OBTAINED FROM AIRBORNE IMAGERY FOR $Cx + c$ AND $Ca + b$ ESTIMATION WITH MODELS OBTAINED THROUGH SCALING UP FOR *P. sylvestris* SAMPLES. SIMULATIONS WERE CONDUCTED WITH PROSPECT-5 COUPLED WITH THREE INFINITIVE REFLECTANCE FORMULATIONS ($R_{\infty 1}; R_{\infty 2}; R_{\infty 3}$) AND DART

CANOPY APPROXIMATIONS		**PROSPECT-5 +$R_{\infty 1}$**		**PROSPECT-5 +$R_{\infty 2}$**		**PROSPECT-5 +$R_{\infty 3}$**		**PROSPECT-5 +DART**	
Regression models for the estimation of *Cx+c* and *Ca+b* content	Equation	R^2	RMSE ($\mu g/cm^2$)	R^2	RMSE ($\mu g/cm^2$)	R^2	RMSE ($\mu g/cm^2$)	R^2	RMSE ($\mu g/cm^2$)
$Cx+c=f((R_{515}/R_{570}; R_{515}/R_{570})^2; R_{750}/R_{710})$	1b	0.66	2.12	0.66	2.09	0.69	1.45	0.66	1.35
$Cx+c=f((R_{515}/R_{570}; R_{515}/R_{570})^2;$ TCARI/OSAVI)	1c	0.66	4.25	0.66	4.24	0.59	1.94	0.60	3.7
$Ca+b=f(R_{750}/R_{710}; (R_{750}/R_{710})^2)$	2b	0.71	9.04	0.71	8.95	0.69	5.5	0.70	4.41
$Ca+b=f$(TCARI/OSAVI; (TCARI/OSAVI)^2)	2c	0.40	33.59	0.40	32.75	0.36	14.91	0.38	22.42

TABLE VII
COEFFICIENTS OF DETERMINATION AND RMSE OBTAINED FROM AIRBORNE IMAGERY FOR $Cx + c$ AND $Ca + b$ ESTIMATION WITH MODELS OBTAINED THROUGH SCALING UP FOR *P. nigra* SAMPLES. SIMULATIONS WERE CONDUCTED WITH PROSPECT-5 COUPLED WITH THREE INFINITIVE REFLECTANCE FORMULATIONS ($R_{\infty 1}; R_{\infty 2}; R_{\infty 3}$) AND DART

CANOPY APPROXIMATIONS		**PROSPECT-5 +$R_{\infty 1}$**		**PROSPECT-5 +$R_{\infty 2}$**		**PROSPECT-5 +$R_{\infty 3}$**		**PROSPECT-5 +DART**	
Regression models for the estimation of Cx+c and Ca+b content	Equation	R^2	RMSE ($\mu g/cm^2$)	R^2	RMSE ($\mu g/cm^2$)	R^2	RMSE ($\mu g/cm^2$)	R^2	RMSE ($\mu g/cm^2$)
$Cx+c=f((R_{515}/R_{570}; R_{515}/R_{570})^2; R_{750}/R_{710})$	1b	0.45	1.82	0.44	1.79	0.37	1.17	0.44	1.46
$Cx+c=f((R_{515}/R_{570}; R_{515}/R_{570})^2;$ TCARI/OSAVI)	1c	0.33	3.21	0.33	3.2	0.39	1.45	0.38	2.74
$Ca+b=f(R_{750}/R_{710}; (R_{750}/R_{710})^2)$	2b	0.72	14.28	0.69	14.17	0.72	3.75	0.72	5.58
$Ca+b=f$(TCARI/OSAVI; (TCARI/OSAVI)^2)	2c	0.67	38.73	0.67	37.89	0.68	18.93	0.1	26.94

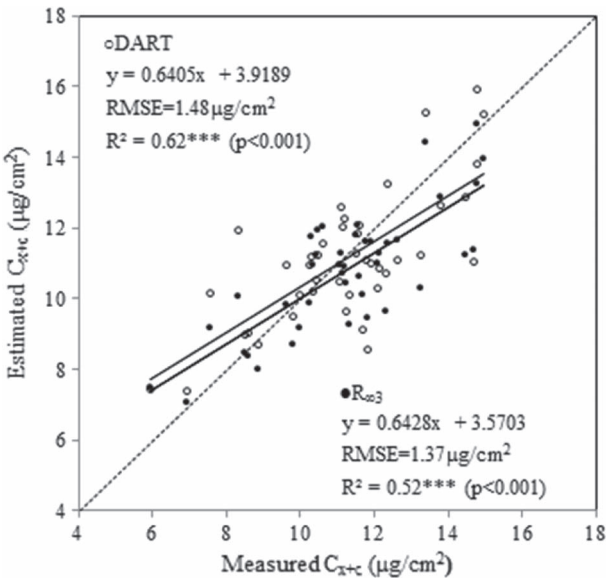

Fig. 7. Validation results obtained for the estimation of $Cx + c$ from airborne hyperspectral imagery using the R_{515}/r_{570} and red edge indices based on an infinite formulation ($R_{\infty 3}$) and DART.

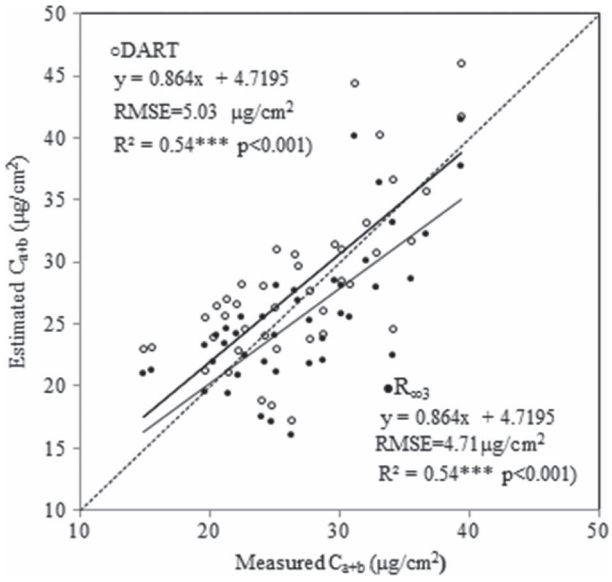

Fig. 8. Validation results obtained for the estimation of $Ca + b$ from airborne hyperspectral imagery using the red edge index based on an infinite formulation ($R_{\infty 3}$) and DART.

Consistently, the results obtained for Black pine stands (see Table VII) were similar between infinite reflectance models and DART. For this species, the $R_{\infty 3}$ approach using the R_{515}/R_{570} and R_{750}/R_{710} indices yielded slightly better results, with RMSE $= 3.75$ μg/cm^2 for $Ca + b$ (15.36%) and RMSE $= 1.17$ μg/cm^2 for $Cx + c$ (21.245%). In agreement with the results obtained for Scotch pine, the use of such models introducing the TCARI/OSAVI index yielded poorer RMSE

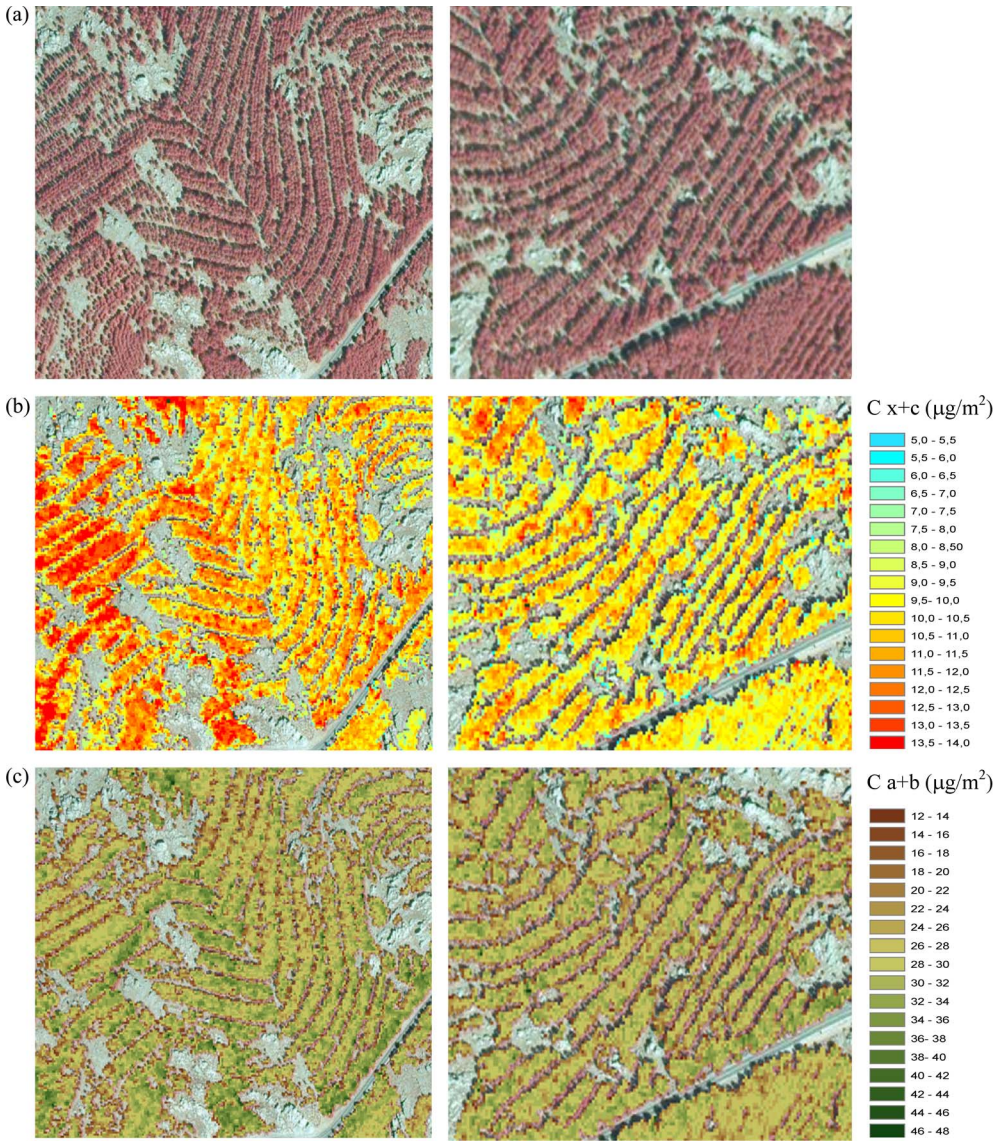

Fig. 9. Mapping results obtained from two samples of *P. sylvestris* and *P. nigra* forest acquired with the AHS hyperspectral imager in a sample area with (left) high and (right) low concentration of chlorophyll and carotenoid pigments. (a) Color infrared image. (b) $Cx + c$ content estimated from the R_{515}/R_{570} and R_{700}/R_{750} indices using $R_{\infty 3}$. (c) $Ca + b$ content estimated from the R_{700}/R_{750} index using $R_{\infty 3}$.

values for Black pine, ranging from 18.93 to 26.94 μg/cm^2 for $Ca + b$ and from 1.45 to 2.74 μg/cm^2 for $Cx + c$ (see Table VII).

Among the data analyzed for both species, Figs. 7 and 8 show the relationships between image-estimated and field-measured $Cx + c$ and $Ca + b$ pigment retrieval, respectively. In both cases, the lowest RMSE was obtained with the $R_{\infty 3}$ model. For the estimation of $Cx + c$, the RMSE obtained with the $R_{\infty 3}$ model was 1.37 μg/cm^2 (17.45%), while DART, $R_{\infty 1}$, and $R_{\infty 2}$ yielded higher RMSE values (RMSE $= 1.48$ μg/cm^2 (17.45%), 2.00 μg/cm^2 (18.30%), and RMSE $= 1.97$ μg/cm^2 (18.20%), respectively). For the estimation of $Ca + b$, the RMSE obtained with the $R_{\infty 3}$ model was 4.71 μg/cm^2 (14.07%) while DART, $R_{\infty 1}$, and $R_{\infty 2}$ yielded higher RMSE values (RMSE $=$ 5.03 μg/cm^2 (13.25%), 11.95 μg/cm^2 (28.89%), and RMSE $=$ 11.85 μg/cm^2 (28.90%), respectively).

The higher performance of $R_{\infty 3}$ in forest canopies agrees with the results obtained by Gitelson *et al.* [12], who demonstrated that model inversion using $R_{\infty 3}$ + PROSPECT showed lower RMSE compared to SAILH + PROSPECT using R_{750}/R_{710} in the merit function if high-resolution imagery was available. It is worth noting the high performance obtained in forest canopies with simpler infinite reflectance models based on Hapke's approach compared to the results obtained with more complex and computationally expensive approaches. These results may be explained by the fact that pure-crown reflectance was extracted based on the high resolution of the images; therefore, soil and shadow effects had a lower influence on target reflectance. The prediction models assessed and applied at image level using object-based methods enabled the mapping of $Cx + c$ and $Ca + b$ with both the R_{515}/R_{570} and R_{750}/R_{710} vegetation indices acquired from the AHS hyperspectral imagery (see Fig. 9). Mapping results made it possible to estimate both pigments at the crown level for the entire scene showing the spatial variability of carotenoid content, with areas with high $Cx + c$ content and low $Cx + c$ content (see Fig. 9).

IV. Discussion

This paper provides insight into the quantification of chlorophyll and carotenoid content simultaneously on conifer forest canopies using scaling-up approaches and narrow-band indices. The major advantage of the methodology used is that it avoids the overlapping problems between wavebands that absorb both pigments (450–550 nm range) [36]. Moreover, $Ca+b$ and $Cx+c$ values are usually strongly correlated. Therefore, a number of carotenoid indices appear to be sensitive to chlorophyll as well. In order to avoid this problem, the improved retrieval of carotenoids and chlorophyll content was obtained by combining two narrow-band indices: the R_{515}/R_{570}, sensitive to $Cx+c$ and proposed by Holder *et al.* [15] for Scotch pine sites, and the red edge index (R_{750}/R_{710}), sensitive to $Ca+b$. In the latter case, the optical indices evaluated and related to $Ca+b$ have been analyzed by other authors [11], [16], [17], [23] for conifer forests. This paper demonstrated that better results were obtained when considering the R_{750}/R_{710} index for $Ca+b$. This result may be explained by the higher effect that tree shadow pixels produce on the TCARI/OSAVI index. This agrees with the result by Zarco-Tejada *et al.* [21], who demonstrated that the TCARI/OSAVI index is highly affected by direct soil background and shadow components, although these results differ from the relationship obtained between the TCARI/OSAVI and canopy $Ca+b$ content for herbaceous and open-tree orchard canopies [18], [21], [22]. By contrast, successful results were obtained with the R_{750}/R_{710} index by Moorthy *et al.* [16], who analyzed $Ca+b$ content using hyperspectral observations in Jack Pine stands, and by Zarco-Tejada *et al.* [11], who studied the same pigment in sugar maple stands.

The estimation of pigment composition in forest canopies using scaling-up methods implies the analysis of the potential confounding effects of open canopy structures on narrow-band vegetation indices. For this reason, the use of complex 3-D radiative transfer modeling was developed to simulate heterogeneous forest canopies [35]. However, the results presented in this paper show that simpler canopy approximations can be also applied targeting pure-crown spectral information. It is relevant to emphasize that $R_{\infty 1}$ and $R_{\infty 2}$ perform better with synthetic data, whereas $R_{\infty 3}$ and DART canopy model approximations perform better applied on experimental data. This suggests that DART and $R_{\infty 3}$ produce simulations that are significantly more realistic than $R_{\infty 1}$ and $R_{\infty 2}$ models. Those results might be related to the different assumptions considered regarding the scattering properties and complexity of thick canopies.

These results agree with those obtained by Zarco-Tejada *et al.* [37], who demonstrated the feasibility of scaling-up methods based on the infinite reflectance approach for crops. In fact, the accuracy of scaling-up methods applied to achieve $Ca+b$ and $Cx+c$ estimations based on infinite reflectance approaches is remarkable. Despite our efforts analyzing complex 3-D radiative transfer models to include the structural variations found in conifer forests, simpler approaches $(R_{\infty 3})$ yielded similar results. This was due to the fact that very high resolution was used to extract pure-crown reflectance from high spatial resolution hyperspectral imagery, removing mixed pixels, shadows, and background effects. It is important to highlight that the forest canopy analyzed in this paper had a relatively low heterogeneity, as it was the product of a systematic afforestation with very low species mix. Therefore, the results obtained with the infinite reflectance approach and the DART simulation analysis might vary in other types of canopies, where the identification of pure crowns is more complicated due to the vegetation mixture or structural heterogeneity of the canopy. This implies that further studies should be carried out in more complex forest canopies comparing different simulation reflectance approaches as a function of varying pixel resolutions.

So far, the methodology proposed in this paper for the simultaneous quantification of both pigments ($Ca+b$ and $Cx+c$) is especially relevant when vegetation stress is addressed. This enables the assessment of the spatial and temporal variations of those pigments previously demonstrated to be related to forest decline processes [8], [9]. Moreover, an accurate spatial quantification of pigment content estimations is presented in this paper using high-resolution hyperspectral image information. Therefore, the methodology proposed in this paper for the simultaneous estimation of both pigments is likely to be useful to analyze spatial and temporal declining physiological states.

V. Conclusion

This paper builds on previous work focused on indices related to carotenoid content estimation. In this paper, scaling-up and predictive relationships were developed using radiative transfer models. Our results demonstrated the feasibility of simultaneously estimating needle $Ca+b$ and $Cx+c$ with scaling-up methods using hyperspectral airborne reflectance data acquired from conifer canopies. These results were obtained based on the scaling up of pure-crown vegetation indices related to chlorophyll (R_{750}/R_{710}) and carotenoids (R_{515}/R_{570}) by using modeling simulations conducted with infinite reflectance models based on Hapke's model coupled with PROSPECT-5. The modeling and experimental results were obtained using the R_{515}/R_{570} and R_{750}/R_{710} vegetation indices for the simultaneous estimation of $Cx+c$ and $Ca+b$. The better performance of the R_{750}/R_{710} index as compared to the TCARI/OSAVI index for chlorophyll content retrieval in forest canopies was probably due to the greater shadow effects of a heterogeneous architecture such as a forest stand on the TCARI/OSAVI. The accuracy obtained by applying scaling-up methods that used simpler approaches such as the infinite reflectance formulation proposed by Hapke was comparable to more complex canopy reflectance approximations such as the DART model. This was due to the very high resolution imagery used, which enabled pure-crown identification. Under these conditions, the modeling analysis and experimental measurements were conducted for the simultaneous estimation of pigment content at the crown level, yielding mean errors of 1.37 μg/cm^2 (17.45%) for $Cx+c$ retrieval and 4.71 μg/cm^2 for $Ca+b$ retrieval (14.07%). In addition, the promising results obtained with 3-D model simulation demonstrate the suitability of this methodology for more complex forest canopies. More complex models such as the 3-D DART canopy reflectance

model estimated $Ca + b$ and $Cx + c$ content slightly more accurately than simpler infinite reflectance models; they showed mean absolute errors of 1.48 μg/cm^2 (17.45%) for $Cx + c$ retrieval and 5.03 μg/cm^2 for $Ca + b$ retrieval (13.25%) but required a considerably larger number of inputs. The generation of biochemical maps at the crown level could play a critical role in the early detection of forest decline processes, enabling the application of such models in precision forestry.

ACKNOWLEDGMENT

The authors would like to thank J. E. Granados and the members of the German-Spanish Astronomical Center (CAHA) at Calar Alto, R. Sanchez and D. Ariza (Evaluación y Restauración de Sistemas Agrícolas y Forestales), and E. Gil-Pelegrín and J. J. Peguero-Pina (Centro de Investigación y Tecnología Agroalimentaria, Zaragoza) for providing technical support during the fieldwork campaigns. The authors would also like to thank J. P. Gastellu-Etchegorry for the support with the discrete-anisotropic-radiative-transfer 3-D radiative transfer model.

REFERENCES

[1] G. A. Carter and R. L. Miller, "Early detection of plant stress by digital imaging within narrow stress-sensitive wavebands," *Remote Sens. Environ.*, vol. 50, no. 3, pp. 295–302, Dec. 1994.

[2] O. Lillesaeter, "Spectral reflectance of partly transmitting leaves: Laboratory measurements and mathematical modeling," *Remote Sens. Environ.*, vol. 12, no. 3, pp. 247–254, Jul. 1982.

[3] F. Batič, P. Kalan, H. Kraigher, H. Šircelj, P. Simončič, N. Vidergar-Gorjup, and B. Turk, "Bioindication of different stresses in forest decline studies in Slovenia," *Water, Air Soil Pollut.*, vol. 116, no. 1/2, pp. 377–382, Nov. 1999.

[4] R. Hernández-Clemente, R. M. Navarro-Cerrillo, L. Suárez, F. Morales, and P. J. Zarco-Tejada, "Assessing structural effects on PRI for stress detection in conifer forests," *Remote Sens. Environ.*, vol. 115, no. 9, pp. 2360–2375, Sep. 2011.

[5] M. Lippert, K. Steiner, H. D. Payer, S. Simons, C. Langebartels, and H. Sandermann, "Assessing the impact of ozone on photosynthesis of European beech (*Fagus sylvatica* L.) in environmental chambers," *Trees*, vol. 10, no. 4, pp. 268–275, Apr. 1996.

[6] T. Hoshizaki, B. N. Rock, and S. K. S. Wong, "Pigment analysis and spectral assessment of spruce trees undergoing forest decline in the NE United States and Germany," *GeoJournal*, vol. 17, no. 2, pp. 173–178, Sep. 1988.

[7] R. Matyssek, M. S. Günthardt-Goerg, T. Keller, and C. Scheidegger, "Impairment of gas exchange and structure in birch leaves (*Betula pendula*) caused by low ozone concentrations," *Trees*, vol. 5, no. 1, pp. 5–13, Apr. 1991.

[8] T. Batič, Z. Užarevic, L. Grgic, J. Roša, and Z. Popovic, "Chlorophylls and carotenoids in needles of damage fir (*Abies alba* Mill.) from Risnjak National Park in Croatia. Acta biologica cracoviensia," *Acta Biol. Cracov.*, vol. 45, no. 2, pp. 87–92, Jun. 2003.

[9] R. Oren, K. S. Werk, N. Buchmann, and R. Zimmermann, "Chlorophyll-nutrient relationships identify nutritionally caused decline in *Picea abies* stands," *Can. J. Forest Res.*, vol. 23, no. 6, pp. 1187–1195, Jun. 1993.

[10] R. Main, M. A. Cho, R. Mathieu, M. O'Kennedy, M. A. Ramoelo, and S. Koch, "An investigation into robust spectral indices for leaf chlorophyll estimation," *ISPRS J. Photogramm. Remote Sens.*, vol. 66, no. 6, pp. 751–761, Nov. 2011.

[11] P. J. Zarco-Tejada, J. R. Miller, G. H. Mohammed, T. L. Noland, and P. H. Sampson, "Scaling-up and model inversion methods with narrow-band optical indices for chlorophyll content estimation in closed forest canopies with hyperspectral data," *IEEE Trans. Geosci. Remote Sens.*, vol. 39, no. 7, pp. 1491–1507, Jul. 2001.

[12] A. A. Gitelson, Y. Zur, O. B. Chivkunova, and M. N. Merzlyak, "Assessing carotenoid content in plant leaves with reflectance spectroscopy," *J. Photochem. Photobiol. B, Biol.*, vol. 75, no. 3, pp. 272–281, Mar. 2002.

[13] J. Peñuelas, I. Filella, and J. A. Gamon, "Assessment of photosynthetic radiation use efficiency with spectral reflectance," *New Phytol.*, vol. 131, no. 3, pp. 291–296, Nov. 1995.

[14] R. Hernández-Clemente, R. M. Navarro-Cerrillo, and P. J. Zarco-Tejada, "Carotenoid content estimation in an heterogeneous conifer forest using narrow-band indices and PROSPECT+DART simulations," *Remote Sens. Environ.*, vol. 127, pp. 298–315, Dec. 2012.

[15] D. N. H. Holder, M. Dockray, and J. Barber, "The red edge of plant leaf reflectance," *Int. J. Remote Sens.*, vol. 4, no. 2, pp. 273–278, Jan. 1983.

[16] I. Moorthy, J. R. Miller, and T. L. Noland, "Estimating chlorophyll concentration in conifer needles with hyperspectral data: An assessment at the needle and canopy level," *Remote Sens. Environ.*, vol. 112, no. 6, pp. 2824–2838, Jun. 2008.

[17] Q. Zhang, X. Xiao, B. Braswell, E. Linder, F. Baret, and B. Moore, "Estimating light absorption by chlorophyll, leaf and canopy in a deciduous broadleaf forest using MODIS data and a radiative transfer model," *Remote Sens. Environ.*, vol. 99, no. 3, pp. 357–371, Nov. 2005.

[18] D. Haboudane, J. R. Miller, N. Tremblay, P. J. Zarco-Tejada, and L. Dextraze, "Integrated narrow-band vegetation indices for prediction of crop chlorophyll content for application to precision agriculture," *Remote Sens. Environ.*, vol. 81, no. 2/3, pp. 416–426, Aug. 2002.

[19] G. Rondeaux, M. Steven, and F. Baret, "Optimization of soil-adjusted vegetation indices," *Remote Sens. Environ.*, vol. 55, no. 2, pp. 95–107, Feb. 1996.

[20] F. Meggio, P. J. Zarco-Tejada, L. C. Núñez, G. Sepulcre-Cantó, M. R. Gonzalez, and P. Martin, "Grape quality assessment in vineyards affected by iron deficiency chlorosis using narrow-band physiological remote sensing indices," *Remote Sens. Environ.*, vol. 114, no. 9, pp. 1968–1986, Sep. 2010.

[21] P. J. Zarco-Tejada, J. R. Miller, A. Morales, A. Berjón, and J. Agüera, "Hyperspectral indices and model simulation for chlorophyll estimation in open-canopy tree crops," *Remote Sens. Environ.*, vol. 90, no. 4, pp. 463–476, Apr. 2004.

[22] P. J. Zarco-Tejada, A. Berjón, R. López-Lozano, J. R. Miller, P. Martín, V. Cachorro, M. R. González, and A. Frutos, "Assessing vineyard condition with hyperspectral indices: Leaf and canopy reflectance simulation in a row-structured discontinuous canopy," *Remote Sens. Environ.*, vol. 99, no. 3, pp. 271–287, Nov. 2005.

[23] P. J. Zarco-Tejada, J. R. Miller, J. Harron, B. Hu, T. L. Noland, N. Goel, G. H. Mohamme, and P. H. Sampson, "Needle chlorophyll content estimation through model inversion using hyperspectral data from boreal conifer forest canopies," *Remote Sens. Environ.*, vol. 89, no. 2, pp. 189–199, Jan. 2004.

[24] B. Pinty, J. L. Widlowski, M. Taberner, N. Gobron, M. M. Verstraete, M. Disney, P. Lewis, F. Gascon, J. P. Gastellu, L. Jiang, X. Li, L. Su, S. Tang, H. Wang, J. Wang, G. Yan, H. Zang, A. Kuusk, T. Nilson, W. Ni-Meister, P. North, W. Qin, R. Thompson, and W. Verhoef, "RAdiation Transfer Model Intercomparison (RAMI) exercise: Results from the second phase," *J. Geophys. Res. D, Atmos.*, vol. 109, no. D6, pp. D06210-1–D0621019, Mar. 2004.

[25] B. Hapke, *Theory of Reflectance and Emittance Spectroscopy*. Cambridge, U.K.: Cambridge Univ. Press, 1993.

[26] N. Yamada and S. Fujimura, "Non-destructive measurement of chlorophyll pigment content in plant leaves from three-color reflectance and transmittance," *Appl. Opt.*, vol. 30, no. 27, pp. 3964–3973, Sep. 1991.

[27] P. R. J. North, "Three dimensional forest light interaction model using a Monte Carlo method," *IEEE Trans. Geosci. Remote Sens.*, vol. 34, no. 4, pp. 946–956, Jul. 1996.

[28] N. S. Goel and R. L. Thompson, "A snapshot of canopy reflectance models and a universal model for the radiation regime," *Remote Sens. Rev.*, vol. 18, no. 2–4, pp. 197–225, Sep. 2000.

[29] J. B. Feret, C. François, G. P. Asner, A. A. Gitelson, R. E. Martin, L. P. R. Bidel, S. L. Ustin, G. le Maire, and S. Jacquemoud, "PROSPECT-4 and 5: Advances in the leaf optical properties model separating photosynthetic pigments," *Remote Sens. Environ.*, vol. 112, no. 6, pp. 3030–3043, Jun. 2008.

[30] J. P. Gastellu-Etchegorry, E. Martin, and F. Gascon, "DART: A 3-D model for simulating satellite images and studying surface radiation budget," *Int. J. Remote Sens.*, vol. 25, no. 1, pp. 73–96, Jan. 2004.

[31] Z. Malenovsky, L. Homolova, P. Cudlin, R. Zurita Milla, M. E. Schaepman, J. G. P. W. Clevers, E. Martin, and J. P. Gastellu-Etchegory, "Physically-based retrievals of Norway spruce canopy variables from very high spatial resolution hyperspectral data," in *Proc. IEEE IGARSS*, Barcelona, Spain, Jul. 2007, vol. 1, pp. 4057–4060.

[32] R. Sánchez-Salguero, R. Navarro-Cerrillo, T. W. Swetnam, and M. A. Zavala, "Is drought the main decline factor at the rear edge of Europe?: The case of southern Iberian pine plantations?" *Forest Ecol. Manage.*, vol. 271, pp. 158–169, May 2012.

[33] A. Abadía and J. Abadía, "Iron and plant pigments," in *Iron Chelation in Plants and Soil Microorganisms*, L. L. Barton and B. C. Hemming, Eds. San Diego, CA, USA: Academic, 1993, pp. 327–344.
[34] T. P. Dawson, P. J. Curran, and S. E. Plummer, "LIBERTY—Modelling the effects of leaf biochemistry on reflectance spectra," *Remote Sens. Environ.*, vol. 65, no. 1, pp. 50–60, Jul. 1998.
[35] J. P. Gastellu-Etchegorry, V. Demarez, V. Pinel, and F. Zagolski, "Modeling radiative transfer in heterogeneous 3-D vegetation canopies," *Remote Sens. Environ.*, vol. 58, no. 2, pp. 13–156, Nov. 1996.
[36] Y. Zur, A. A. Gitelson, O. B. Chivkunova, and M. N. Merzlyak, "The spectral contribution of carotenoids to light absorption and reflectance in green leaves," in *Proc. 2nd Int. Conf. Geospatial Inf. Agr. Forestry*, Buena Vista, FL, USA, Jan. 10–12, 2000, vol. 2, pp. 1–7.
[37] P. J. Zarco-Tejada, M. L. Guillén-Climent, R. Hernández-Clemente, A. Catalina, M. R. González, and P. Martín, "Estimating carotenoid content in vineyards using high resolution hyperspectral imagery acquired from an Unmanned Aerial Vehicle (UAV)," *Agr. Forest Meteorol.*, vol. 171/172, pp. 281–294, Apr. 2013.

Rocío Hernández-Clemente received the Agricultural Engineering degree and the international Ph.D. degree from the University of Córdoba (UCO), Córdoba, Spain.

Her specific lines of research are focused on the analysis of high-resolution hyperspectral data to estimate leaf biochemical and canopy biophysical variables through leaf and canopy radiative transfer modeling. She is currently with the Treesat Laboratory, UCO, where she has a contract as a Scientific Researcher of the Seventh Framework Programme Thermolidar project based on the application of advanced technologies and new methods to improve estimates of structural information and physiological variables in forestry based on the fusion of airborne LiDAR with thermal data sets.

Rafael Maria Navarro-Cerrillo received the degree in forest engineering and the Ph.D. degree from the School of Agricultural Engineering and Forestry of Madrid, Madrid, Spain.

He is currently a Professor with the University of Córdoba, Córdoba, Spain, and the Head of the ERSAF research group. He has more than 25 years of experience on forestry science. He has 20 years of working experience in silviculture, restoration, and remote sensing. He has participated in different international projects in Europe, Latin America, and Asia.

Pablo J. Zarco-Tejada received the degree in agricultural engineering from the University of Córdoba, Córdoba, Spain, the M.Sc. degree in remote sensing from the University of Dundee, Scotland, U.K., and the Ph.D. degree in earth and space science from York University, Toronto, ON, Canada.

He has been a contract faculty member for remote sensing at the University of California, Davis, CA, USA. He works on hyperspectral data to estimate biochemical and canopy biophysical variables through leaf and canopy modeling and the effects of chlorophyll fluorescence. He is currently with the Institute for Sustainable Agriculture, Spanish Council for Scientific Research, Córdoba.